

SYNTHESIS AND SPECTROSCOPIC CHARACTERIZATION OF ANATASE TiO₂ NANOPARTICLES

Ahmed A. Hussain and *Hilal S. Wahab

^aDepartment of Chemistry, College of Science, Al-Nahrain University, PO Box 64090, Al-Jadriya, Baghdad, Iraq.

ABSTRACT

Titanium dioxide nanoparticles are used in various applications including environmental photocatalysis and solar cells. In this work we present the synthesis of TiO₂ nanoparticles employing sol-gel methodology. The morphology, composition, particle size, surface area and band gap of these nanoparticles have been characterized and compared with a standard anatase TiO₂ reference specimen exploiting several instrumental techniques namely, Scanning Electron Microscopy (SEM), Energy Dispersive X-Ray Spectroscopy (EDXS), X-Ray Diffraction (XRD), Diffused Reflectance UV-VIS spectrometry (DUR-UV-VIS), Transmission Electron Microscopy (TEM), Brunauer–Emmett–Teller (BET) theory and Raman Spectrometry.

Key Words: Titanium oxide; Anatase; Nanoparticles; Spectroscopy; Characterization

INTRODUCTION

Considerable attention has been paid on the synthesis and application of nanocrystalline materials, because of their novel and spectacular physical and chemical properties. These particular properties are resulted from the ultrafine structures (i.e., grain sizes smaller than 50 nm) of these materials and can be classified in two categories: properties that are relative to the bulk and to the surface^[1].

Over the years, a large number of nanocrystalline semiconductors have been used as photocatalysts. The most commonly studied catalyst is TiO₂, ZnO, SnO₂ and CdS^[2]. Titanium dioxide has become the bench mark and the most suitable catalyst against which photocatalytic activity of other semiconductors is measured because of its high oxidizing ability, long-term stability, low cost and no toxicity^[3].

TiO₂ exists naturally as rutile, anatase and brookite allotropes. Rutile appears to be the most common form of TiO₂, while anatase and brookite forms of TiO₂ tend to convert into rutile form upon heating at high temperature.

*Corresponding author :

hswahab@gmail.com

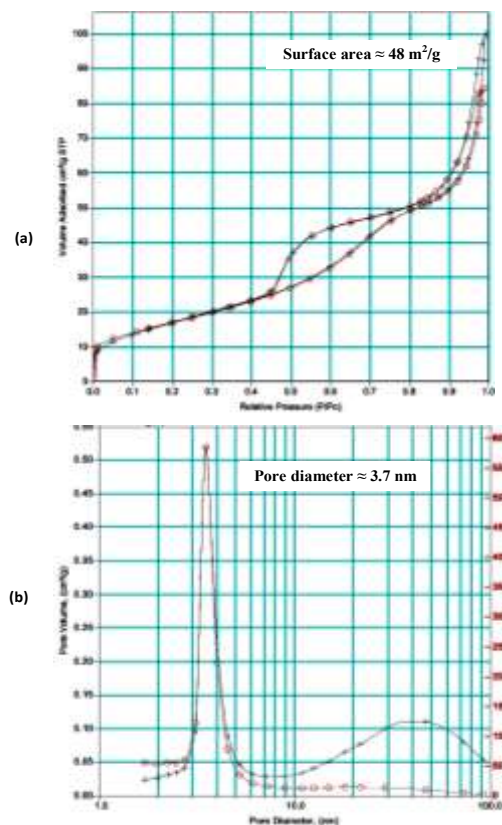


Fig. 1. BET measurements for nano anatase TiO₂ ; (a) Isotherm plot and (b) pore size plot.

TiO₂ is well known for its widespread applications in paints, sunscreens, environmental treatment and purification purposes^[4]. Furthermore, anatase form of TiO₂ has the best photocatalytic activity, followed by

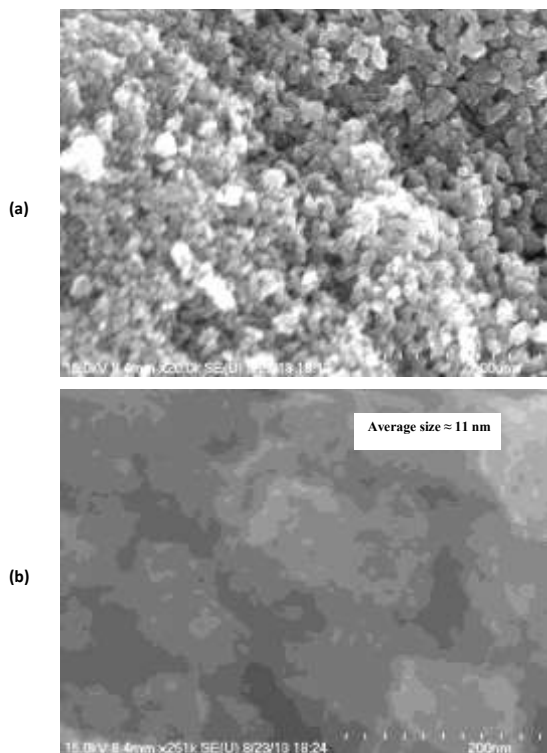


Fig. 2. Scanning Electron Microscope (SEM) images of nano anatase TiO₂ with different sizes; (a) 200 μm and (b) 200 nm.

rutile form. TiO₂ can utilize natural UV radiation from sunlight for photocatalysis because it has suitable energetic separation between its conduction and valence band. Band-gap energy of TiO₂ (3.2 eV for anatase; 3.03 for rutile) is relatively smaller compared to other semiconductors, such as ZnO (3.35 eV) and SnO₂ (3.6 eV). Therefore, TiO₂ is able to absorb photons energy in the near UV range (wave length < 387 nm) and consequently, can be activated by ultraviolet (UV) light and thus utilizes 5% of the solar spectrum^[5].

Meso- and micro-porous nanostructured TiO₂ has received quite a bit of attention and a great amount of work has been performed on TiO₂ over the years and has led to an understanding that is unprecedented for a metal oxide surface^[6,7]. On the other hand, due

to the mixed ionic and covalent bonding in metal oxide systems, the surface structure has presented a strong influence on local surface chemistry as compared to metals semiconductors^[8,9]. Moreover, the

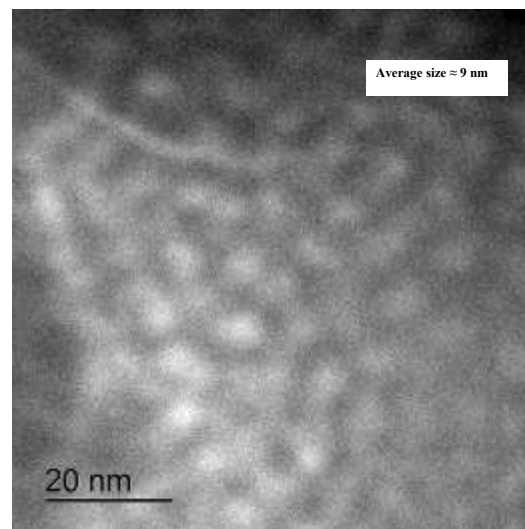


Fig. 3. Transmission Electron Microscope (TEM) image of nano anatase TiO₂ Particles.

nanostructured TiO₂ played a special role due to its large area/volume ratio providing the opportunity for adsorption and consequently photo detoxification of large amounts of organic moieties pollutants on very small amounts of substrate due to the very high specific area of the adsorbent^[10,11]. Generally no single analytical spectroscopic tool can provide adequate information concerning structural and functional features for the nanostructured TiO₂ particles^[12]. Accordingly, various spectroscopic methodologies are desperately required to study the structural and functional characterization. On these bases, this study aimed to synthesize and then systematically characterize size, porosity, surface morphology, composition and band gap energy by a combination of spectroscopic techniques including Scanning Electron Microscopy (SEM), Energy Dispersive X-Ray Spectroscopy (EDXS), X-Ray Diffraction (XRD), Diffused Reflectance UV-VIS spectrometry (DUR-UV-VIS), Transmission Electron Microscopy (TEM), Brunauer–Emmett–Teller (BET) theory and Raman Spectrometry.

EXPERIMENTAL

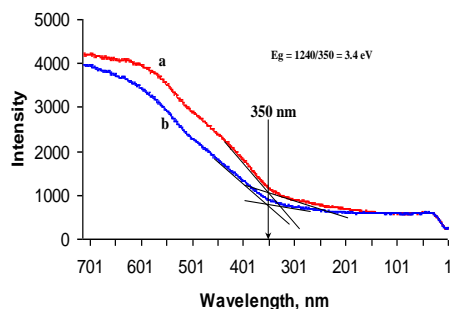


Fig. 4. Diffused reflectance UV-VIS absorption threshold for (a) standard nanopowder anatase TiO_2 reference specimen; (b) synthesized nanopowder anatase TiO_2

Chemicals

All the chemicals which have been used were as high purity as available and used without further purification. Phenol Red (98%, Thomas Baker), Isopropanol (99.8%, Riedel Dehean), Titanium Isopropoxide (98%, Acros Organics) and standard nanopowder anatase TiO_2 reference specimen (particle size < 25 nm, 99.7%, Sigma-Aldrich). Deionized nanofiltered water, DNFW (TDS \approx Zero) was used for all experiments.

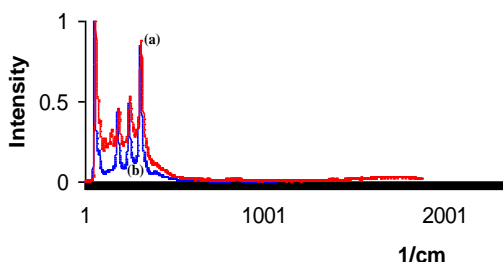


Fig. 6. Raman spectra for (a) standard nanopowder anatase TiO_2 reference specimen; (b) synthesized nanopowder anatase TiO_2

TiO_2 nanoparticle catalyst synthesis

Titanium dioxide nanosized catalyst was synthesized by the sol-gel method by means of a gradual addition of a solution of titanium isopropoxide (5 ml isopropanol + 5 ml titanium isopropoxide) onto 200 ml of DNFW at pH = 5 with a rate of addition of 2 ml / min. The mixture was kept, after completion of addition, under continuous vigorous mixing at room temperature until the completion of hydrolysis (2 hours). The resulting transparent colloidal

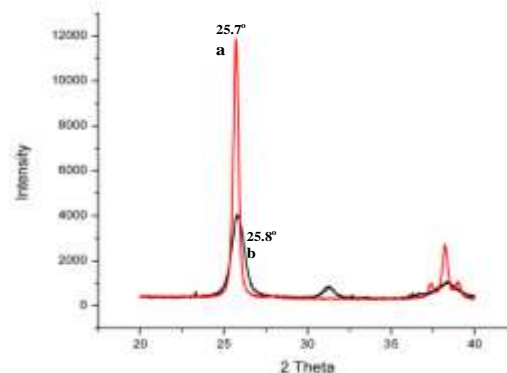


Fig. 5. X-ray Diffraction Spectroscopy (XRD) patterns of (a) standard nanopowder anatase TiO_2 reference specimen; (b) synthesized nanopowder anatase TiO_2

solution was left aging for 24 hours then filtered, dried at $90\text{ }^\circ\text{C}$ for two hours and finally was calcined at $400\text{ }^\circ\text{C}$ for 4 hours. Grinding into fine powder, if needed, overcomes the agglomeration.

For the sake of comparison, the characterization of the synthesized catalyst has been conducted along with standard nanopowder anatase TiO_2 reference specimen (particle size < 25 nm, 99.7%, Sigma-Aldrich).

RESULTS AND DISCUSSION

Surface morphology

The surface area and pore size of the synthesized anatase TiO_2 nanoparticles are measured employing Brunauer.Emmett.Teller (BET) Bel Sorp 18 Plus nitrogen adsorption apparatus after the sample was degassed at $100\text{ }^\circ\text{C}$ for 4 hours. Figure 1a illustrates the adsorption-desorption isotherm plot which results in surface area of $48\text{ m}^2/\text{g}$. Further, Figure 1b shows the maxima at pore size of 3.7 nm, which indicates the mesoporosity of the prepared nano anatase TiO_2 particles. The surface morphology and the approximate particle size of the meso- porous TiO_2 were characterized by a cold field emission high resolution scanning electron microscope (Hitachi S-4700 FE-SEM) at two different magnifications with very smooth and homogeneous surfaces and average size of 11 nm (Figure 2 a and b). The surface has also been explored by high resolution Scanning Transmission Electron Microscope (Hitachi

HT7700 STEM) for nanoscale analysis. The nanocrystals have an irregular spherical shape and excellent dispersivity with average size of 9 nm (Figure 3). On the other hand it should be noted that the necking regions between the particles are benefit for the formation of network structure as observed in SEM and TEM images which is expected to be advantageous for the transport of electron in the skeleton ^[1]. Based on the above results, we may report here that the relatively low calcination temperature (400 C°) is beneficial in preserving the particle size at nano scale.

Energy and composition perspectives

Ground state diffused reflectance absorption spectra of solid powder for both the standard nanopowder anatase TiO₂ reference specimen and synthesized nanopowder anatase TiO₂ were collected using Avantes / Ava spec 2048 Diffused UV-VIS Reflectance Spectroscopie equipped with a 300 watt Xe-lamp source. Figure 4 depicts explicitly the excellent accordance of absorption thresholds for both the reference and synthesized specimen at 350 nm which subsequently refer to band gap energy (E_g) of 3.4 eV.

The X-ray diffraction (XRD) patterns of the nanoparticles that are presented in Figure 5 have been recorded in Pananalytical Philips diffractometer with Cu K α radiation (0.15425 nm) in the range of 2 θ from 20° to 40°. Diffraction signal assigned to the anatase (101) structure at 25.3° (25.7°-25.8° in this work) is clearly observed in TiO₂ ^[1]. The diffraction signal at 27.5° due to the rutile phase (110) is not observed in TiO₂ powder. on the basis of the above findings, one can conclude that the absence of the diffraction due to the rutile phase in synthesized TiO₂ nano powder proved that the calcination at 400° might be the appropriate temperature for anatase TiO₂ preparation.

The average grain size was calculated by Sherrer's equation using the XRD line broadening method ^[13]. The crystal size $D = 0.9 \lambda / (B \cos \theta)$ where λ represents the wavelength of X-ray, B the FWHM and the θ diffraction angle. By using the experimental data, an average grain size of 9.95 nm was derived,

The peak width inversely proportional with particle size in which by increasing the peak width the size of nano TiO₂ decreases. Accordingly, a closer look at Fig.5 confirms this phenomenon in which the synthesized nano TiO₂ band (Fig. 5b) shows more broadening than the reference TiO₂ band (Fig. 5a) whose grain size is consequently (\approx 25 nm) higher than that of the prepared nano TiO₂ (9.95 nm).

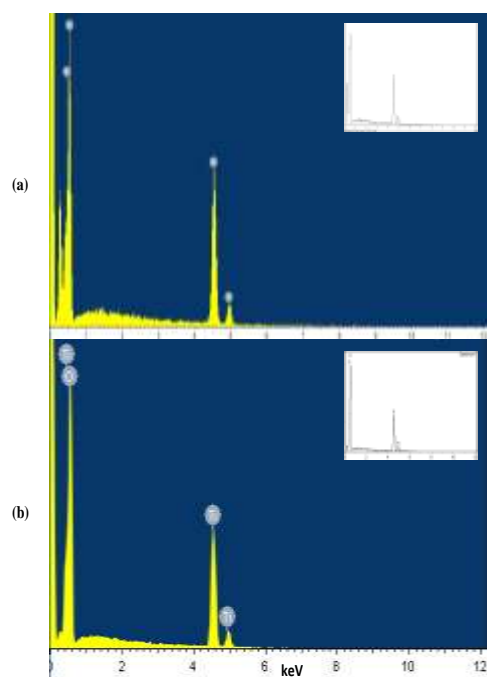


Fig. 7. Energy Dispersive X-ray Spectroscopy (EDXS) image of (a) standard nanopowder anatase TiO₂ reference specimen; (b) synthesized nanopowder anatase TiO₂

For further scrutinization, Raman measurements have also been performed. Figure 6 exhibits a clear matching between the spectra of prepared nano anatase TiO₂ (Fig. 6b) and the reference specimen (Fig. 6a). The spectrometer used for the Raman measurements is a Spex Ramalog 4. The Raman spectra were obtained with an argon-ion laser operating at 4880 Å and 5145 Å with incident power 50 mW. Light scattered at 90° to the incident beam was passed through a double-grating monochromator and detected photoelectrically. Moreover, the wavelength calibration was made using the neon and mercury emission lines.

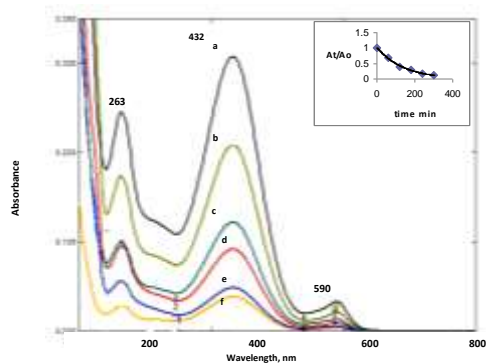


Fig. 8 . UV-VIS spectra changes of Phenol red (10 mg/L) in aqueous nano TiO₂ dispersion (0.53 g/L) irradiated under UV light at varying times: (a) 0, (b) 1, (c) 2, (d) 3, (e) 4 and (f) 5 hours. Inset shows the normalized absorbance at 432 nm.

Prior to the application of the synthesized anatase nano powder on the photo bleaching process of a model pollutant (Phenol Red), the composition of the synthesized nano anatase TiO₂ was verified using Hitachi S-3700N VP-SEM coupled with Energy Dispersive X-ray Spectrometer (EDXS). The spectra shown in Figure 7b (prepared) is to an excellent extent similar to that of reference sample which is shown in Fig. 7a.

The synthesized nano anatase TiO₂ powder was examined in photo bleaching of phenol red as recalcitrant environmental pollutant. Optimum operational conditions namely, pH = 4.5 , nano powder loading = 40 mg, UV light intensity = 485 E-10 Ein / sec. L and pollutant concentration = 10 mg/L have been employed. Figure 8 shows a gradual photo decolorization of the polluted solution over 5 hours of irradiation ending with > 90% degradation. Also from Fig. 8, increasing in the illumination time allows the absorption spectra to be shifted exponentially toward the low absorbance values for the main absorption band , 432 nm, indicating the destruction of its chromophoric structure. This is accompanied by simultaneous decrease of the intensities of other bands, 263 and 590 nm.

CONCLUSIONS

Nanometric anatase TiO₂ powder was successfully prepared by the simple sol gel

method. XRD pattern confirmed the neat anatase allotrope without rutile diffraction peaks stemming from high calcination temperatures. SEM and TEM images revealed smooth and highly dispersive surfaces with average size of 9-11 nm.. The composition resulted has been consistent with that of the reference anatase specimen of TiO₂ as corroborated by EDXS measurements. The bandgap energy as determined from the diffused reflectance spectrum amounted to 3.4eV, which was identical to that recorded for reference TiO₂ sample. BET measurements confirmed the mesoporosity with average surface area of 48 m²/g. Moreover, the evaluation of the synthesized nano photocatalyst resulted in an excellent photo bleaching of the model pollutant, phenol red.

CONFLICT OF INTEREST

Nil

REFERENCES

- [1] Jiu J., Isoda S., Adachi M., Wang F., Preparation of TiO₂ nanocrystalline with 3–5 nm and application for dye-sensitized solar cell, *J. of Photochem. and Photobiol. A: Chemistry* 189, 314–321 (2007).
- [2] Lathasreea S., Nageswara R. A., SivaSankar B., Sadasivam V., Rengaraj K., Heterogeneous photocatalytic mineralisation of phenols in aqueous solutions, *J. of Mol. Catal. A: Chemical* 223, 101–105 (2004).
- [3] Wahab H. S., Bredow T., Aliwi S. M. ,A Computational study on the adsorption and ring cleavage of para-chlorophenol on anatase TiO₂ surface, *Surf. Sci.* 603, 664-669 (2009).
- [4] Teh C. M., Mohamed A. R., Roles of titanium dioxide and ion-doped titanium dioxide on photocatalytic degradation of organic pollutants (phenolic compounds and dyes) in aqueous solutions: A review, *J. of Alloys and Compds* 509, 1648–1660 (2011).

- [5] Song S., Hong F., He Z., Cai Q., Chen J., AgIO₃ modified AgI / TiO₂ composites for photocatalytic degradation of p-chlorophenol under visible light irradiation, *J. of Colloid and Interface Sci.* 378, 159–166 (2012).
- [6] Diebold U., The surface science of titanium dioxide, *Surf. Sci. Rep.* 48, 53-229 (2003).
- [7] Konstantinou I. K., Albanis T.A., TiO₂-assisted photocatalytic degradation of azo dyes in aqueous solution: kinetic and mechanistic investigations: A review, *Appl. Catal. B: Environmental* 49, 1–14 (2004).
- [8] Barteau M. A., Site requirements of reactions on oxide surfaces, *J. Vac. Sci. Technol. A* 11, 2162-2169 (1993).
- [9] Wahab H. S. , Environmental Remediation Modeling; Computational and Experimental Photocatalytic Aspects of Chloroaromatics on Nano Induced TiO₂, Lambert Academic Publishing, Saarbrücken, Germany, 2013.
- [10] Nalwa H. S. in ,Handbook of surfaces and interfaces of materials" vol. 2: surface and interface analysis and properties, Academic Press, 2001.
- [11] Wahab H. S. , Molecular modeling of the adsorption and initial photocatalytic oxidation step for para-nitrophenol on nano-sized Ti surface, *Surf. Sci.* 606, 624-633 (2012).
- [12] Chen J., Gu B., LeBoeuf E., Pan H., Dai S., Spectroscopic characterization of the structural and functional properties of natural organic matter fractions, *Chemosphere* 48, 59-68 (2002).
- [13] Brus L.E., Electron–electron and electron hole interactions in small semiconductor crystallites: The size dependence of the lowest excited electronic state, *J. Chem. Phys.* 80, 4403-4412 (1984)